SMART

SMART Detector Project:

recent results from the SMART experiment

Donato Creanza

Dipartimento Interateneo di Fisica & INFN – Bari

on behalf of the SMART Collaboration

6th International "Hiroshima" Symposium September 11-15, 2006

Introduction

RD48 → RD50

Pad diodes → full size sensors

Within RD50 the need has risen to:

- investigate new materials properties
- test wafers quality and optimize production processes
- check minisensors functionality on promising materials

→ SMART: a collaboration among Bari, Firenze, Perugia, Pisa INFN institutes & ITC-IRST Trento

OXYGEN ENRICHED SILICON

Oxygen getters radiation-induced vacancies: V + O → VO (not harmful at RT)
High oxygen content reduces formation of V_2, V_3, V_2O, V_2O_2,...;
i.e. related deep acceptor levels ⇒ less negative space charge

Recent results on MCz after 24 GeV p irradiation

A) MCz offers the same trapping times [1] and reverse current [2] as standard FZ silicon, but has an improved long term annealing and does not type invert up to $\Phi \sim 10^{15}$n/cm^2, exhibiting a lower stable damage rate β [3].

B) A proper fabrication process does not induce TDs nor change the N_{eff} of substrates [4,5].

C) Similar results have been obtained after 900 MeV e^- irradiation up to $\Phi = 6 \cdot 10^{15}$cm^{-2} [6] and low energy protons up to $5 \cdot 10^{14}$n/cm^2 [7].

[1] A. G. Bates and M. Moll, ”A comparison between irradiated MCz and FZ Si detectors by TCT,” NIM A, in press.
[2] G. Pellegrini et al., NIM A, 552 (2005) 27-33.
[3] G. Segneri et al., ”Radiation hardness of high resistivity n- and p-type magnetic Cz silicon,” NIM A, submitted.
[4] M. Bruzzi et al., NIM A, 552 (2005) pp. 20-26.
[5] G. Pellegrini et al. NIM A, 548 (2005) pp. 355-363.
[6] S. Dittongo et al., NIM A, 546 (2005) 300-305.
[7] J. Harkonen et al., NIM A, 541 (2005) 202-207.

Oxygen concentration in FZ, CZ and EPI

Cz and DOFZ silicon

- **CZ: high O_i (oxygen) and O_{2i} (oxygen dimer) concentration (homogeneous)**
- **CZ: formation of Thermal Donors possible !**

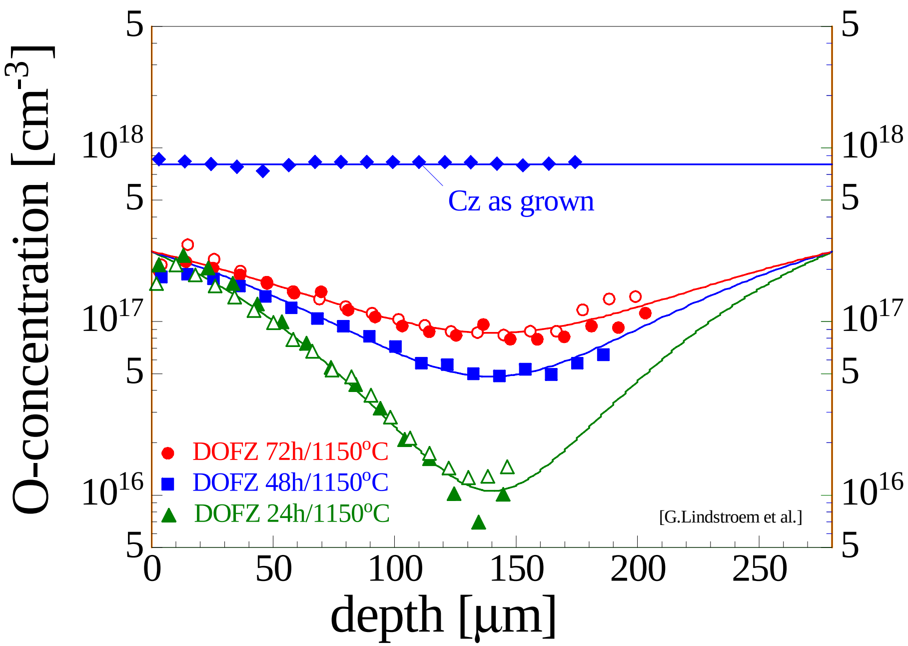

- **DOFZ: inhomogeneous oxygen distribution**
- **DOFZ: oxygen content increasing with time at high temperature**

Epitaxial silicon

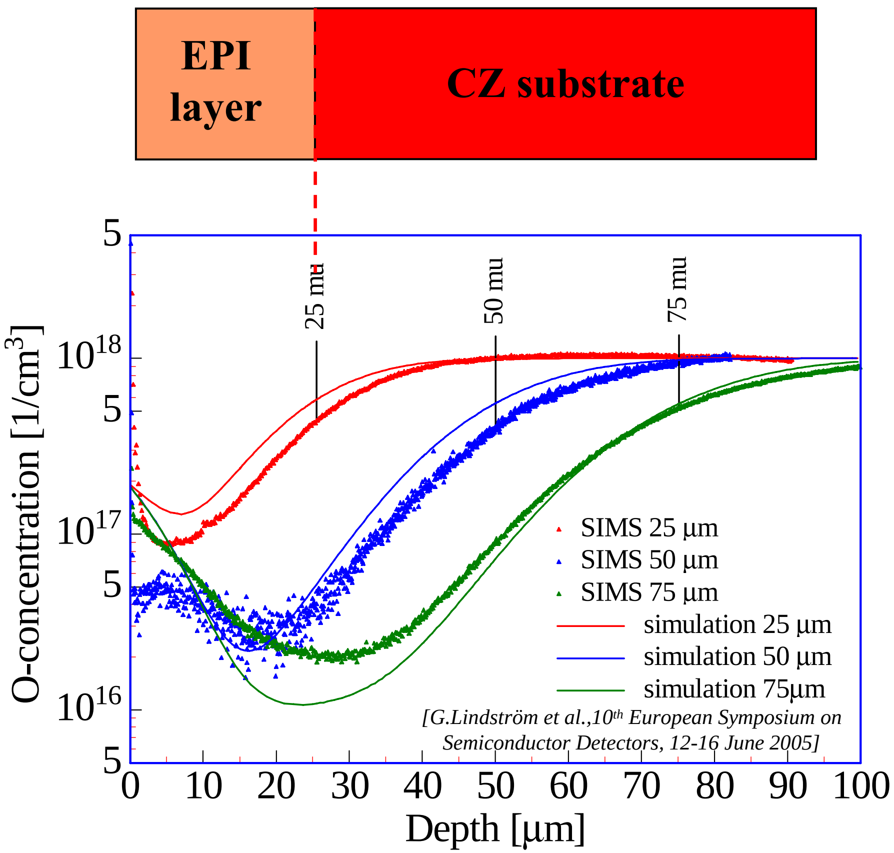

- **EPI: O_i and O_{2i} (?) diffusion from substrate into epi-layer during production**
- **EPI: in-homogeneous oxygen distribution**

n-in-p microstrip detectors

n-in-p: - no type inversion → high electric field stays on structured side
- collection of electrons → less trapping

- **Miniature n-in-p microstrip detectors (280µm)**
- **Detectors read-out with LHC speed (40MHz) chip (SCT128A)**
- **Material: standard (SFZ) and oxygenated (DOFZ) p-type FZ**
- **Irradiation:**

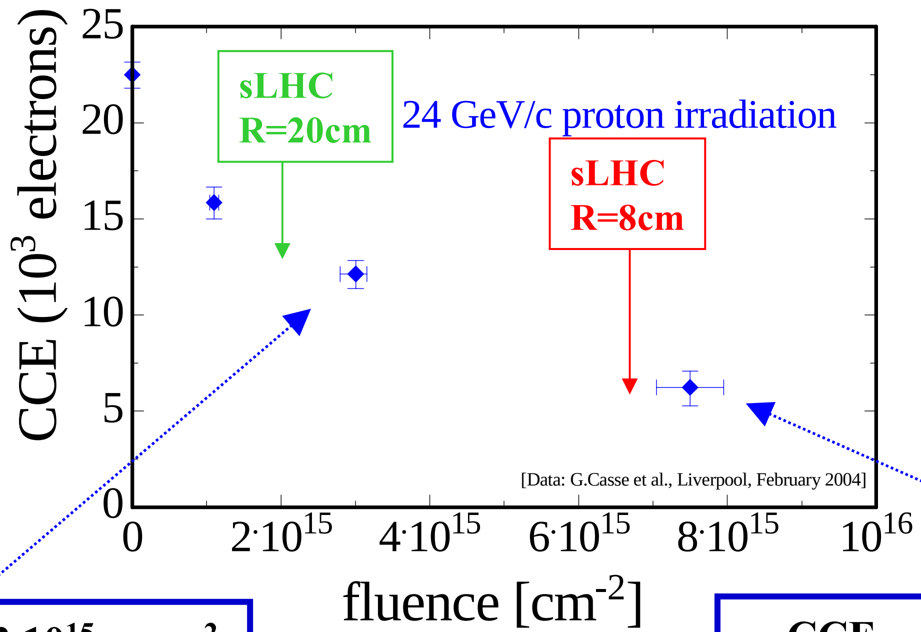

G. Casse et al., NIMA535(2004) 362

At the highest fluence $Q \sim 6500e$ at V_{bias}=900V

CCE ~ 60% after 3 10^{15} p cm^{-2} at 900V(standard p-type)

CCE ~ 30% after 7.5 10^{15} p cm^{-2} 900V (oxygenated p-type)

SMART: Wafer layout, 4”

1st p-type MCz microstrip detectors

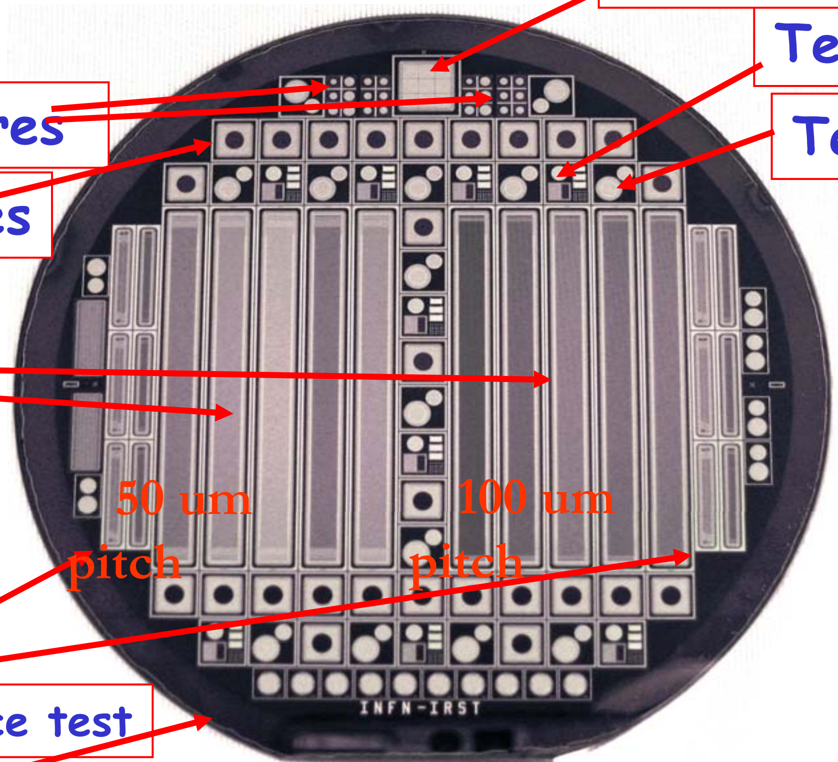

RUN I p-on-n

22 wafers

Fz, MCz, Cz, Epi

RUN II n-on-p

24 wafers Fz, MCz

two p-spray doses:

3E12 & 5E12 cm^{-2}

- ✓RD50 common wafers procurement
- ✓Wafer Layout designed by SMART collaboration
- ✓Masks and process by ITC-IRST (Trento)

Pre-Irradiation Characterization : Diodes

SMART

SMART1 - p^+/n - MCz 300μm

Diode IV: High V_{bd} and good current density

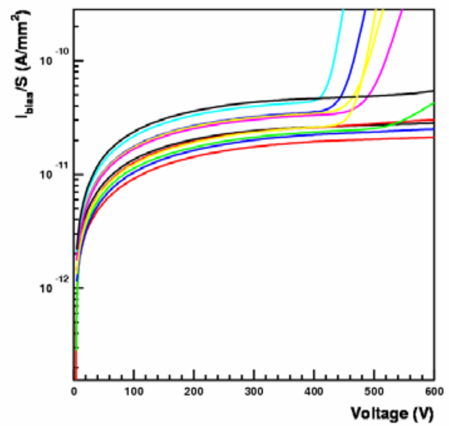

Diode CV: Uniform ρ at wafer level

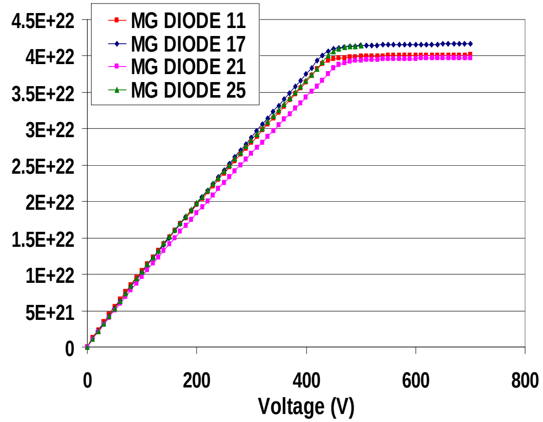

MOS CV : uniform process of the wafers

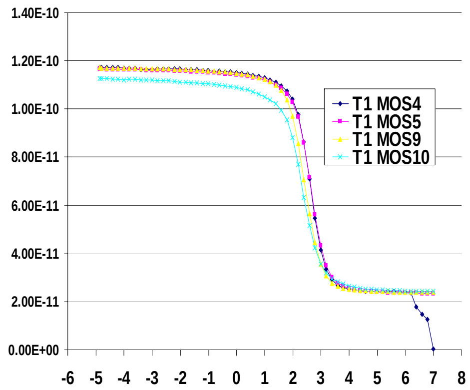

SMART2 - n^+/p - MCz 300μm

Process temperature kept below 400 °C in order to avoid Thermal Donors activation

Map of the diodes V_{FD} in a p-type MCz wafer →

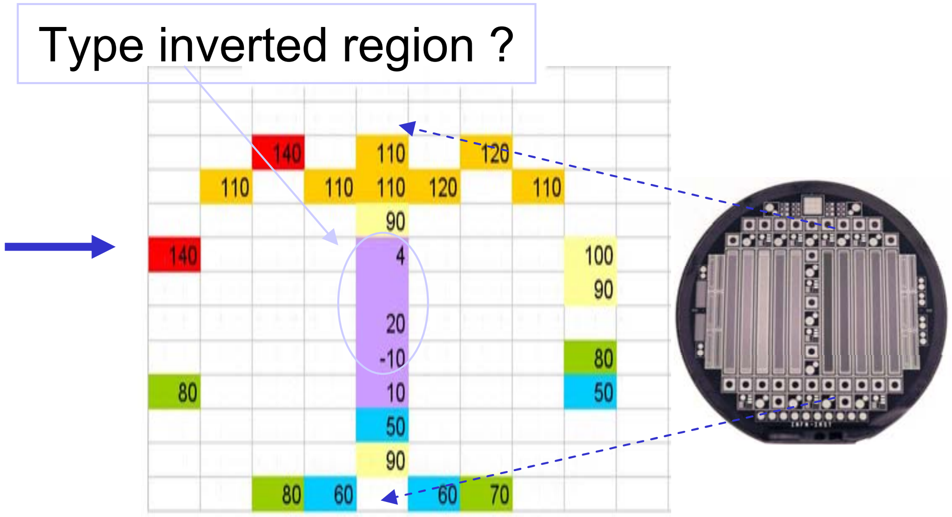

Disuniformity probably due to fluctuations in the oxygen concentration in MCz material

C. Piemonte, 5th RD50 workshop Oct 2004

ρ can be tuned by high temperature (400 °C) annealing

SMART MCz: 24 GeV/c proton irradiation…

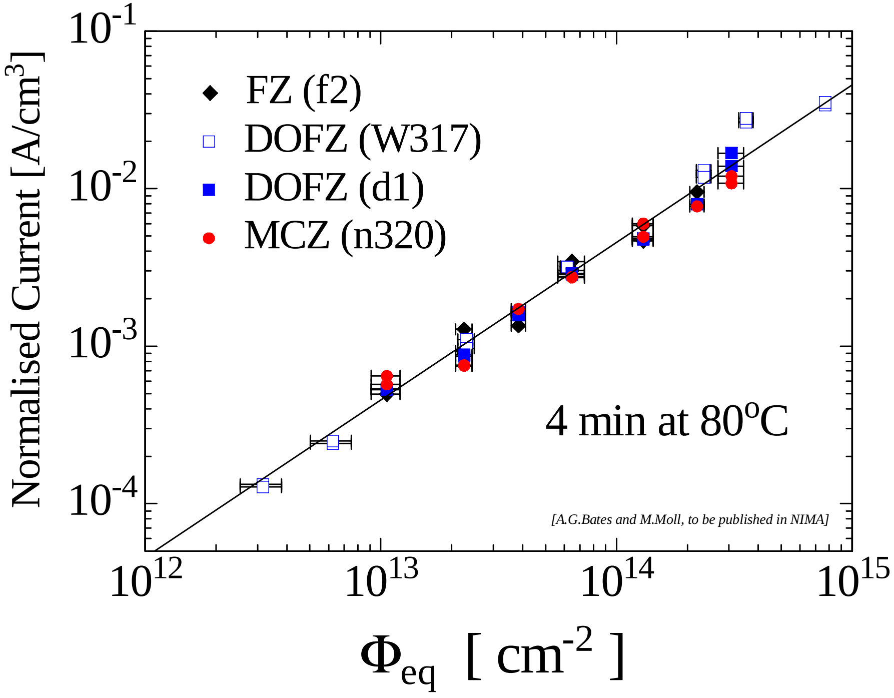

- Depletion voltage extracted from CV, IV and TCT measurements

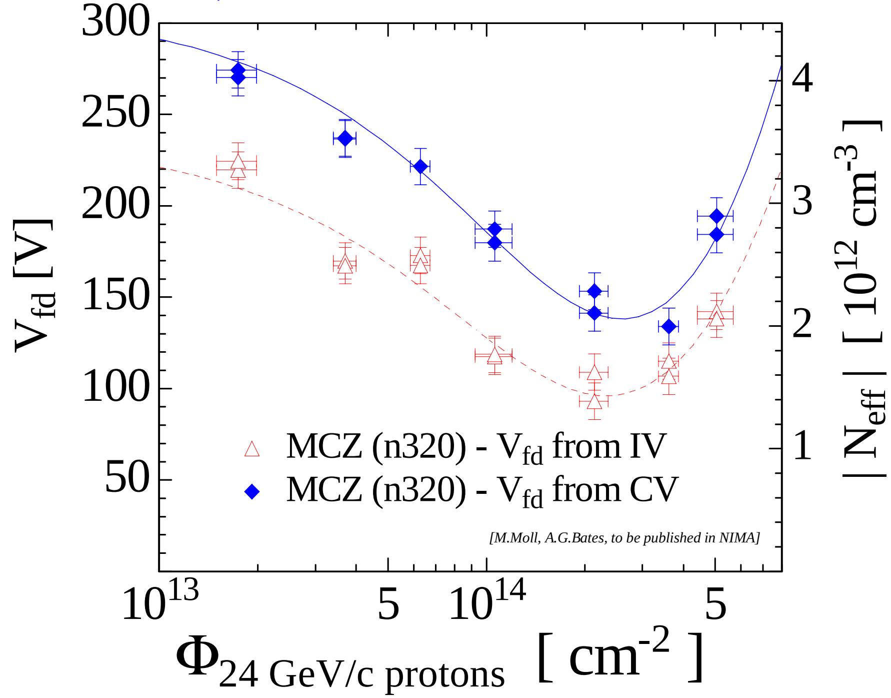

- **Leakage Current :**
  as for DOFZ, FZ (and EPI)

- **Question: is the material type inverted (SCSI) ?**

SMART …and 26 MeV proton irradiation

The annealing behaviour is typical of inverted (p-type) material after $\Phi_4 \approx$1E14:
Does MCz n undergoe type inversion?

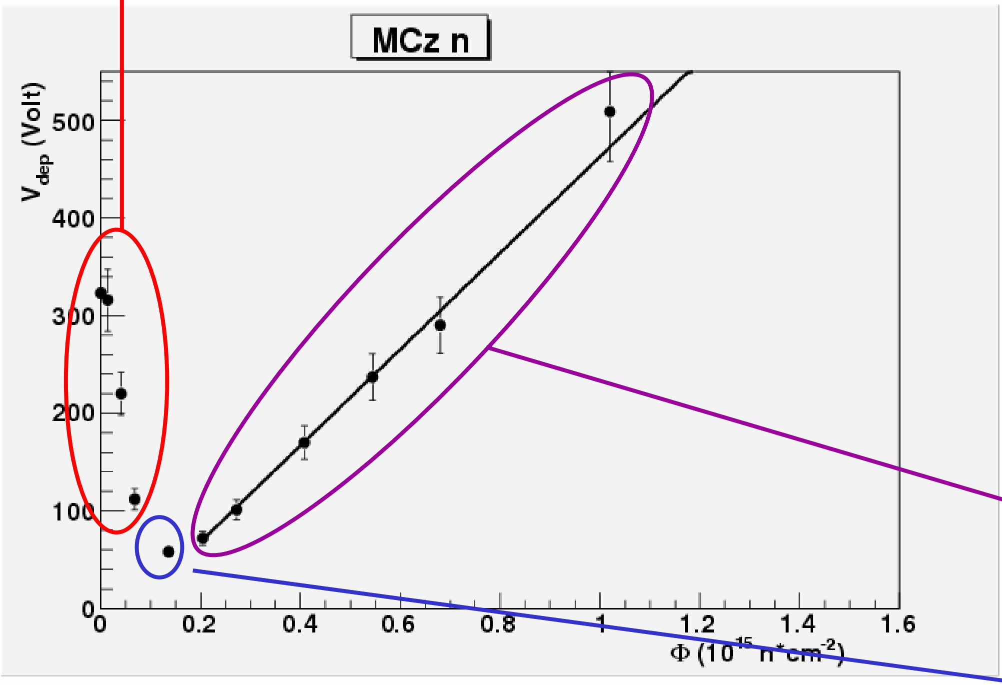

Annealing @ T=20^{0}C

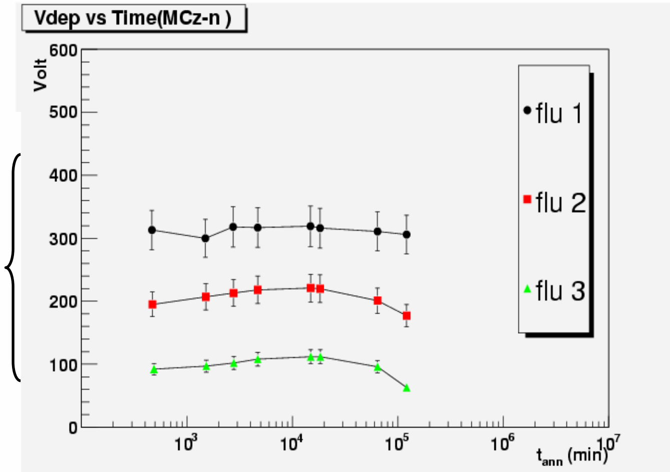

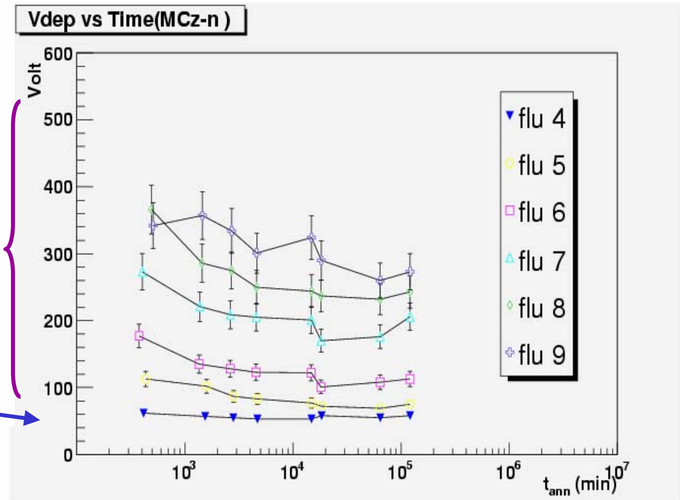

BUT:
- **Minimum of V_{dep} *vs* Φ well above 0V**
- **No SCSI observed for 24 GeV/c p irr.**

Annealing @ 80^0C

SMART

PROTON IRRADIATION

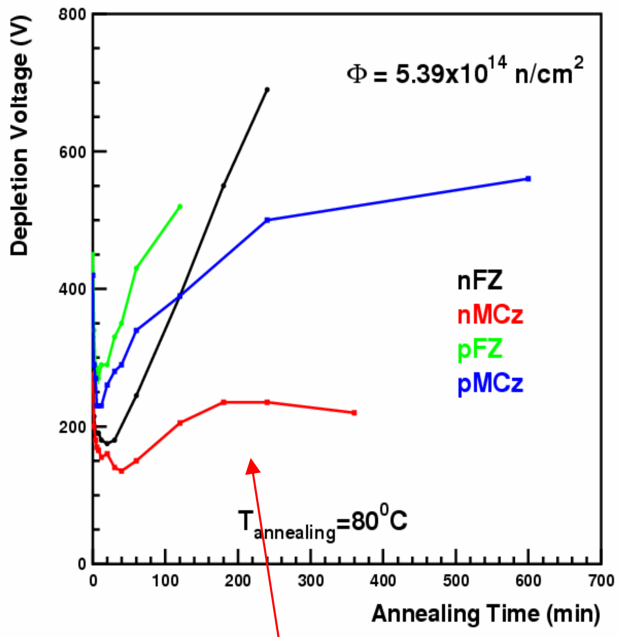

Saturation effect for MCz Si (n & p) beyond 200 minutes at 80 °C

NEUTRON IRRADIATION

Up to 60 min at 80° C

Fz and MCz show the same behavior.

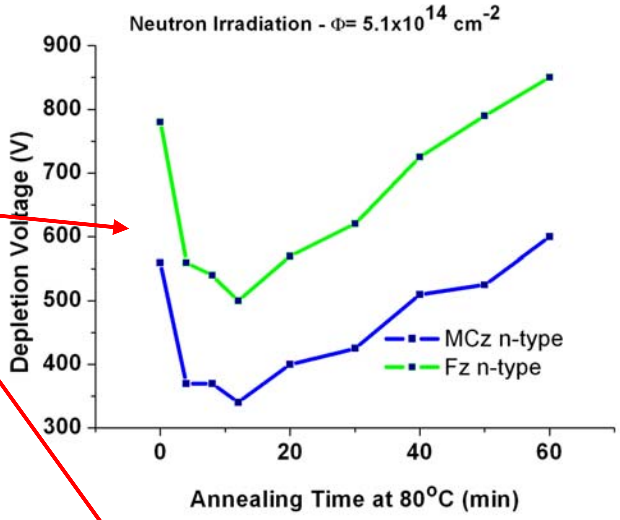

extrapolated

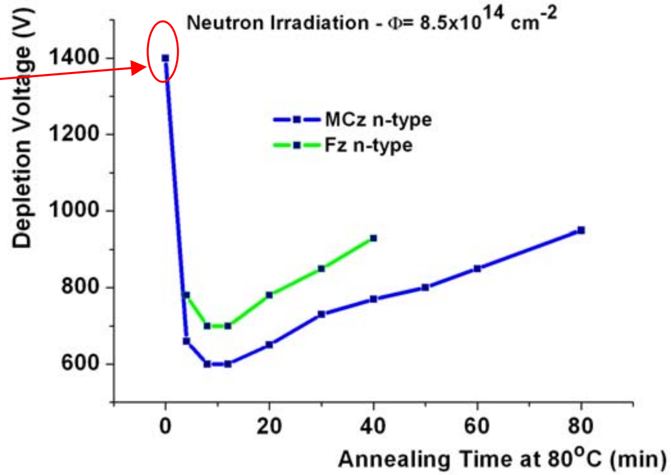

Reverse annealing @ high temperature

Comparison of SFZ and MCz (n- and p-type) @ 80°C:

Effect of reverse annealing significantly reduced in MCz Si after irradiation with 26MeV and 24GeV/c protons up to 2×10^{15} n_{eq} cm^{-2} with respect to FZ Si.

Clear saturation for MCz Si (n or p) beyond 200 minutes at 80 °C

Saturation more effective for n-type

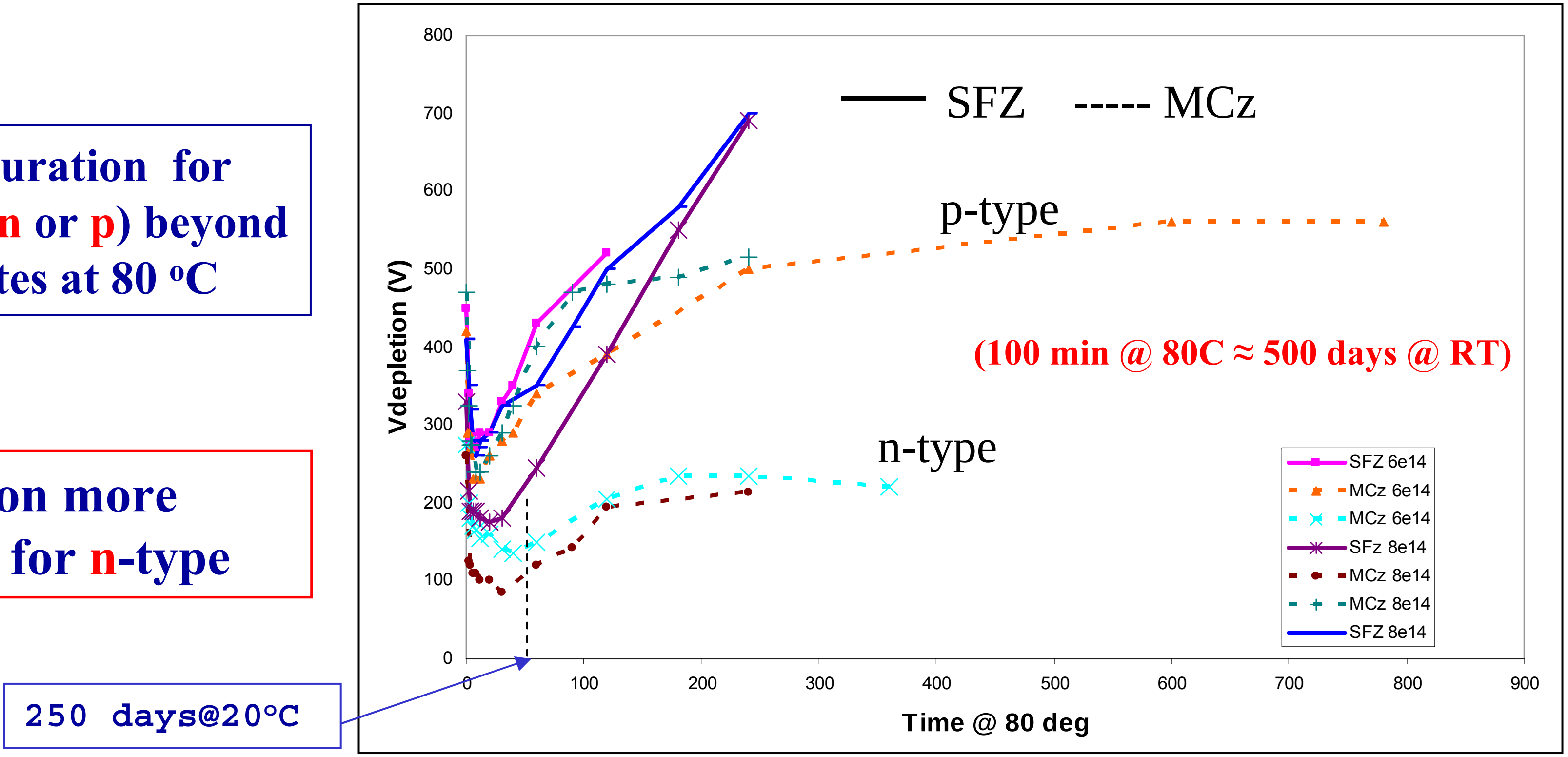

The reduced reverse annealing growth would simplify damage recovery in experimental operational conditions

Epitaxial 150 μm

- Strong increase of the depletion voltage with fluence

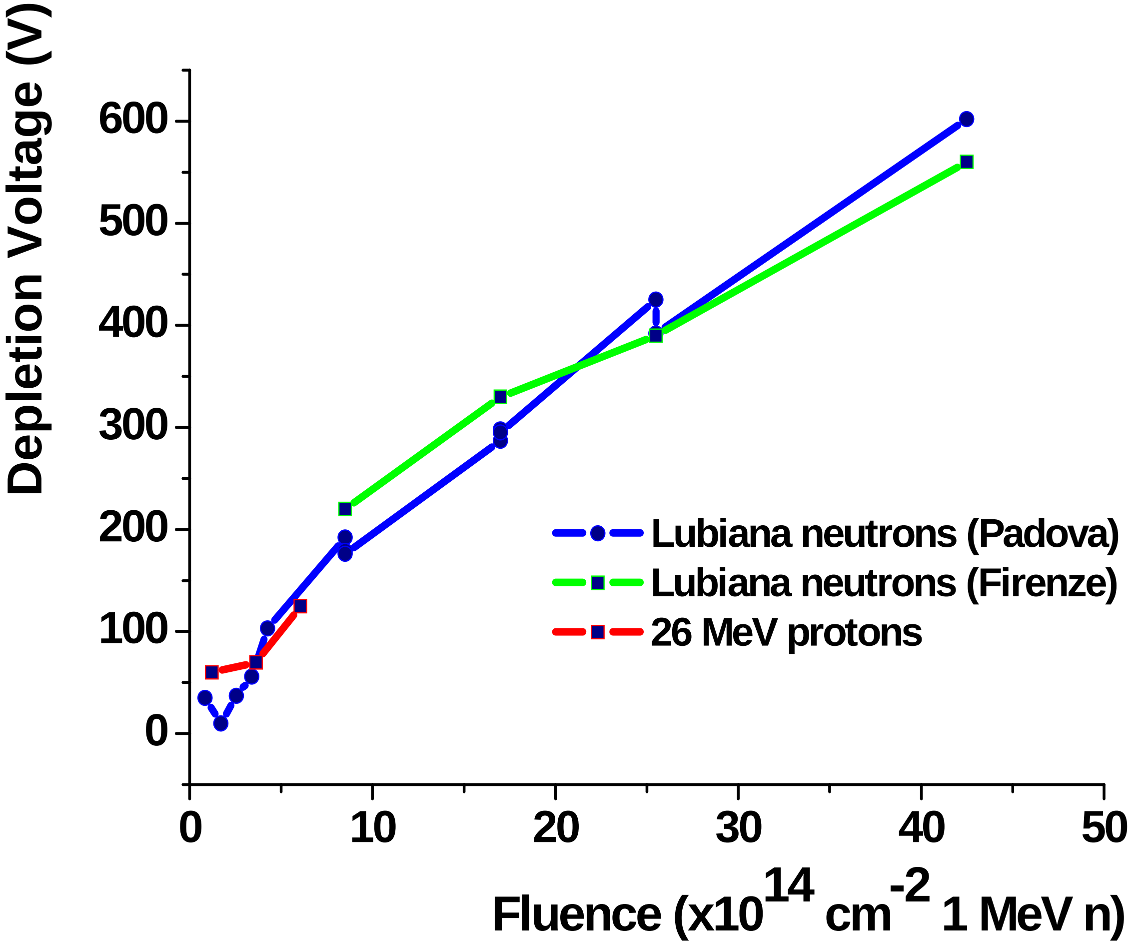

- V_{fd} at the minimum is above 0 V: inversion or double junction effect?

(see next slides)

SMART

Epitaxial diodes: Annealing

INFN Istituto Nazionale di Fisica Nucleare

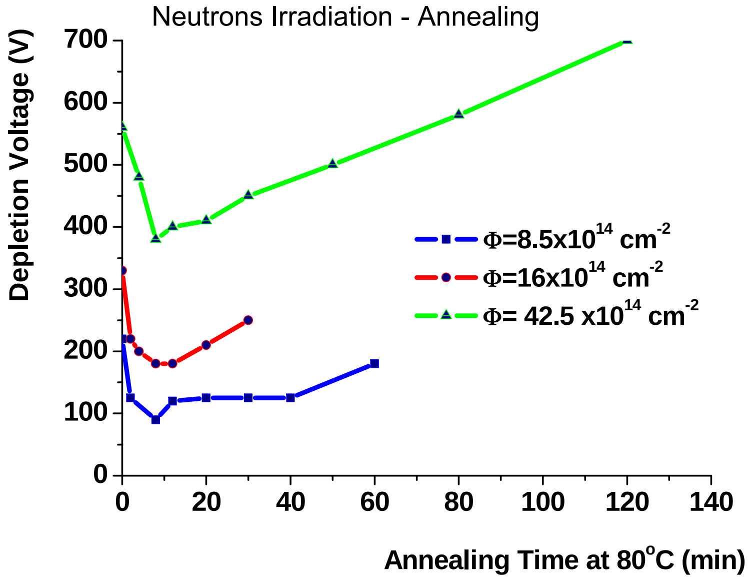

Neutron irradiation: "inverted-like" behaviour

SCSI?

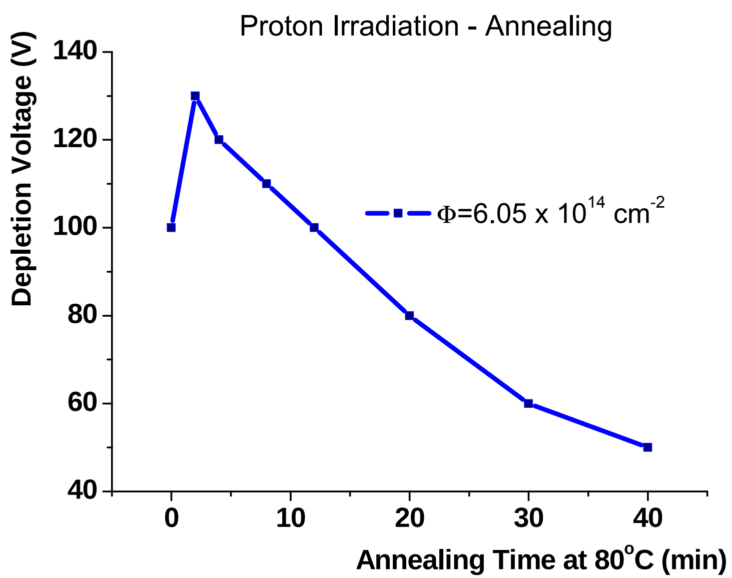

Proton irradiation: "not inverted-like" behaviour

Double Junction (DJ) effect

For very high fluences (of the order of 10^{14} n_{eq}/cm^2) a depletion region can be observed on both sides of the device for STFZ p^+/n diodes. In STFZ DJ arises after inversion. The opposite in MCz! This may explain $V_{dep}(\Phi,t)$ profiles.

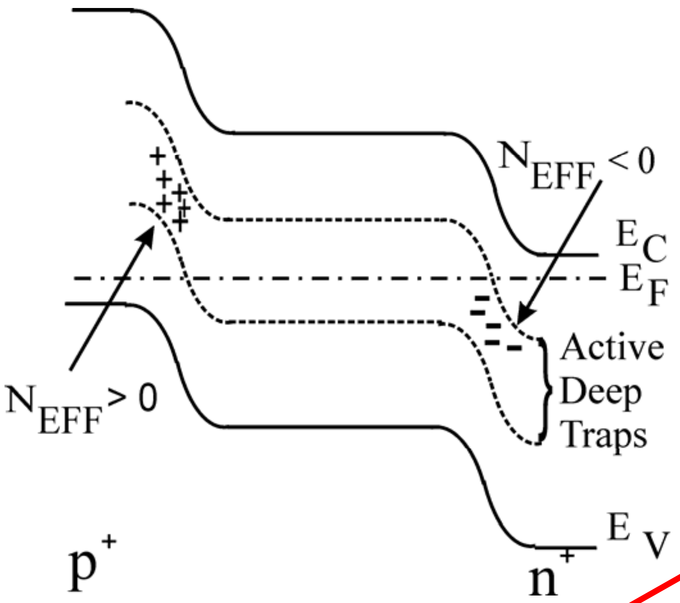

- Double junction effect has been observed on MCz starting from Φ = **3×10^{14}** n_{eq}/cm^2
- At the fluence **Φ=1.3×10^15^** → **$\Phi=1.3\times10^{15}$** n_{eq}/cm^2 the dominant junction is still on the p^+ side for 24 GeV/c protons irr.

Strip readout side: no over depletion

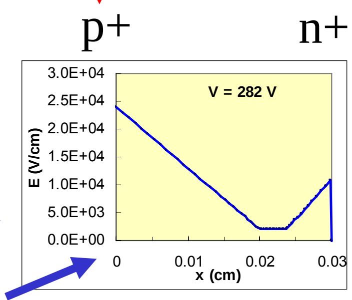

Electric field extracted from fit - TCT data

No SCSI on MCz up to

Φ~1.3×10^15^ n_{eq}/cm^2

TCT measurements

Fake "SCSI" on MCz at Φ~2×10^14^ n_{eq}/cm^2

1. ***Minimum on Vdep vs fluence***
2. ***Slope of annealing curves***

DJ modeling and simulation

SMART

D. Menichelli, 7th RD50 Workshop:

- **A simplified model to study $V_{fd}(N_1,N_2)$ as a function of effective doping on junction: N_1 (p+ side) N_2 (n+ side)**

$V_d \sim (N_1+N_2) - 3N_1N_2/(N_1+N_2))$

Irradiation effect:

$N'_1 = N_{10} - b_1\Phi$

$N'_2 = b_2(\Phi - \Phi_0)$

Φ_0: fluence at which DJ appears

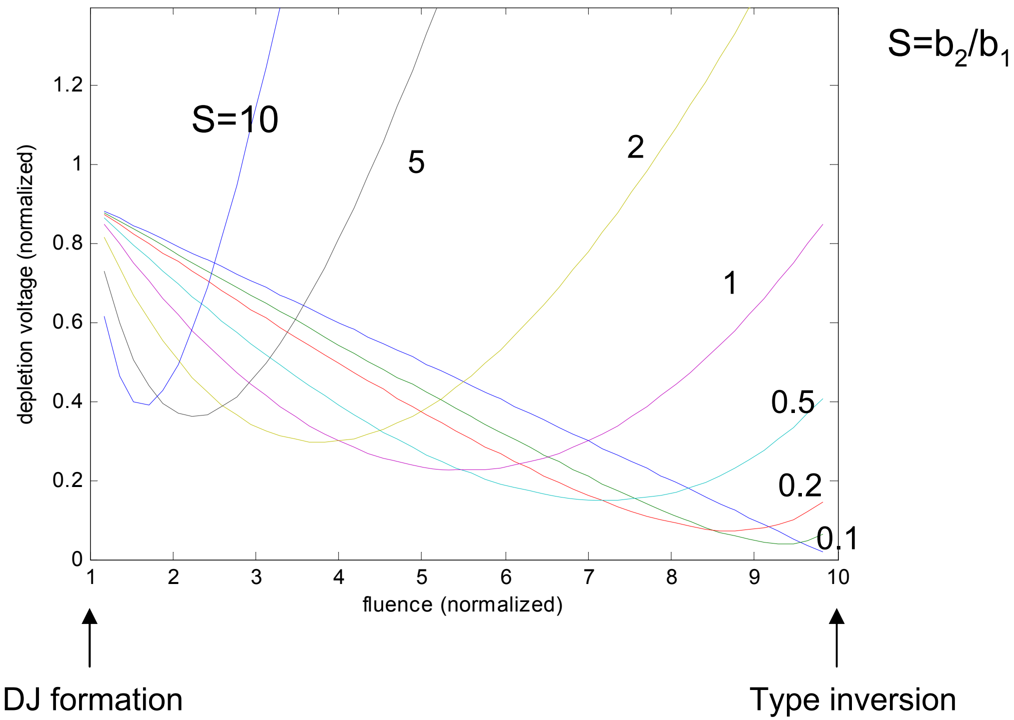

Qualitative agreement between CV/ annealing curves
Systematic investigation under study

SCSI

For **low energy protons** irradiation the mechanism seems to be the same, even if SCSI has been recently observed at high fluences.

Analysis of new TCT measurements made at Joffe PT Institute (S. Petersburg) on irradiated SMART samples is under way. Preliminary results seem to confirm such picture. They also show evidence of SCSI occurence in **MCz** and 150µm thick **EPI** samples irradiated with **neutrons**, in agreement with other recent observations (see G. Kramberger and E. Verbitskaya, 8th RD50 Workshop - Prague, June 2006)

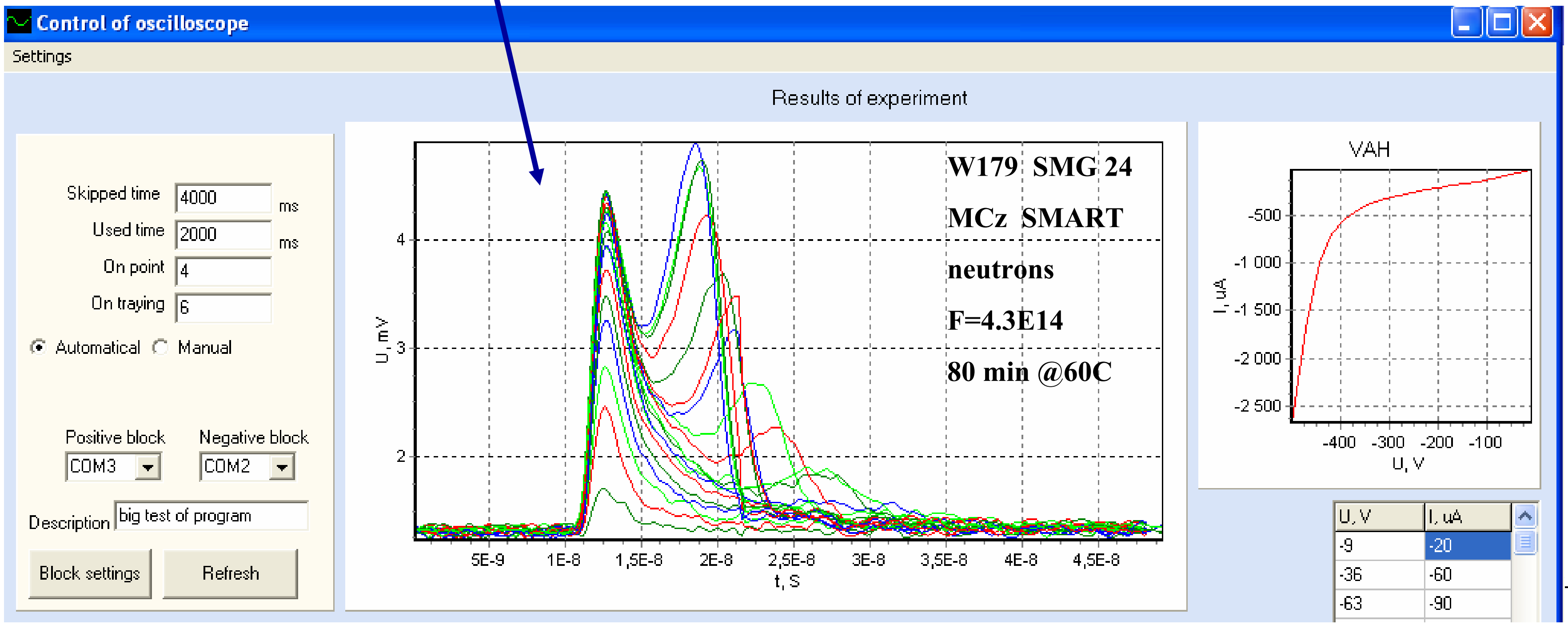

Microstrip detectors characteristics

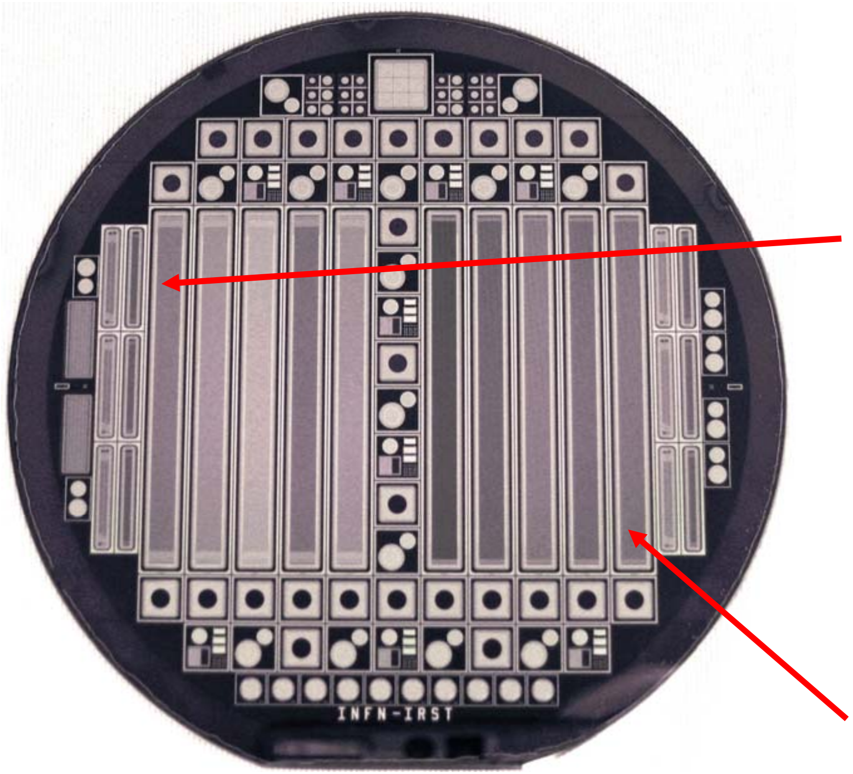

det#	pitch	p^+ implant width	polysilicon width	metal width
	[um]	[um]	[um]	[um]
1	50	15	10	23
2	50	20	15	28
3	50	25	20	33
4	50	15	10	19
5	50	15	10	27
6	100	15	10	23
7	100	25	20	33
8	100	35	30	43
9	100	25	20	37
10	100	25	20	41

Several geometries: pitch, w/p, metal overhang…

Pre-Irradiation Characterization : Minisensors

SMART

SMART1 - p^+/n - MCz 300μm

Good performance of the n-type detectors in terms of breakdown voltages and current uniformity

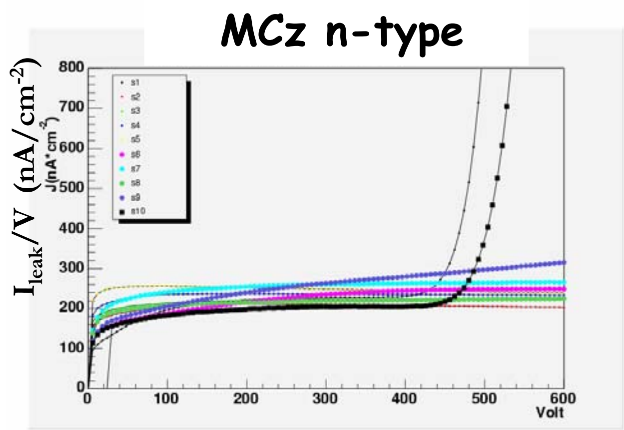

Wafer uniform resistivity, effect of strip geometry on V_{depl} and C_{tot}

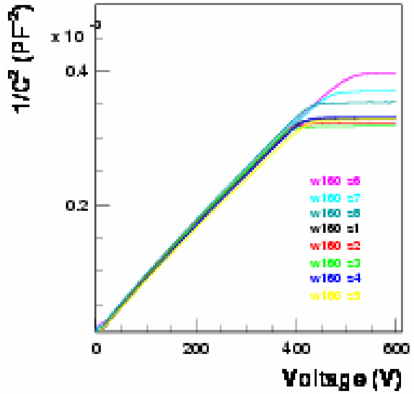

SMART2 - n^+/p - MCz 300μm

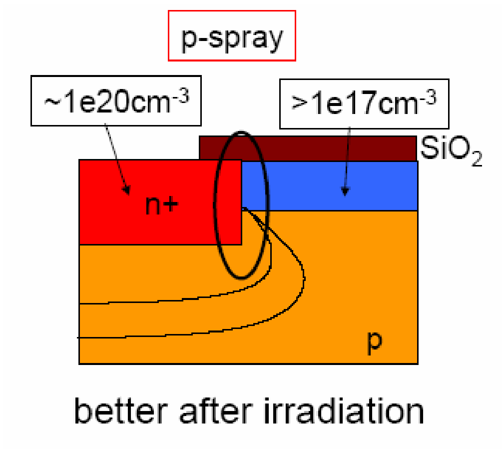

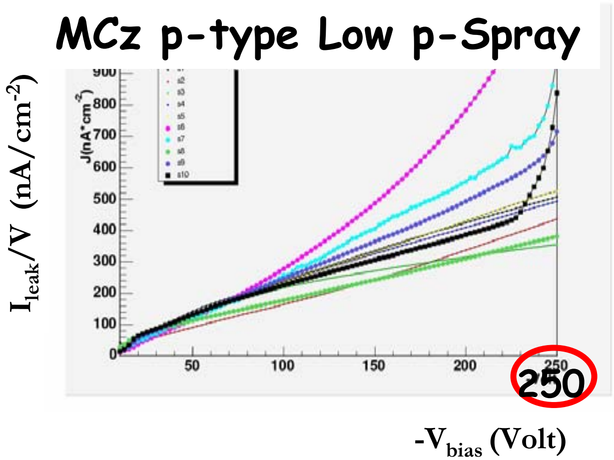

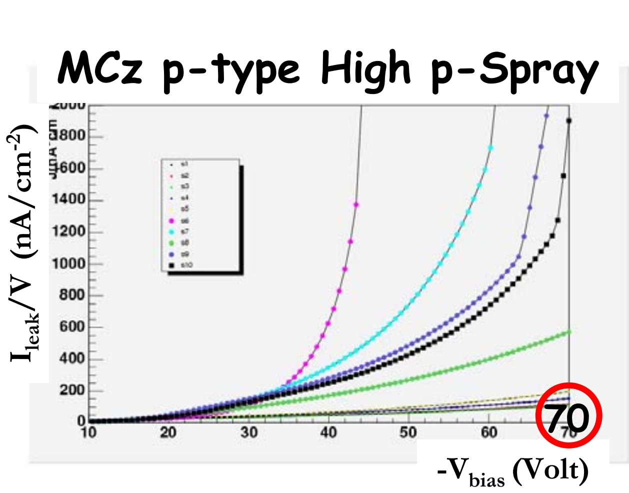

SMART

I_{leak} performance of proton irr. microstrip sensors

n-type

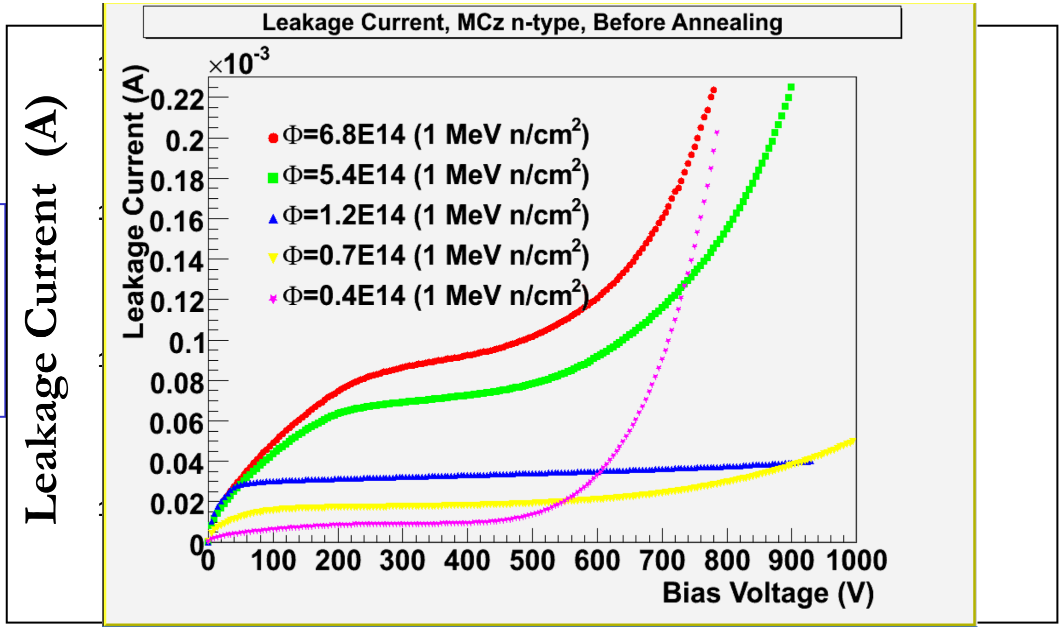

IV curves of n-type detectors for the full fluence range before annealing (measured at 0°C):

(1) Current levels in MCz detectors are comparable with Fz at a given fluence

(2) Leakage currents measured at V_{depl} scale as the received fluences.

The performances of Fz and MCz p-type detectors are much improved after irradiation.

p-type

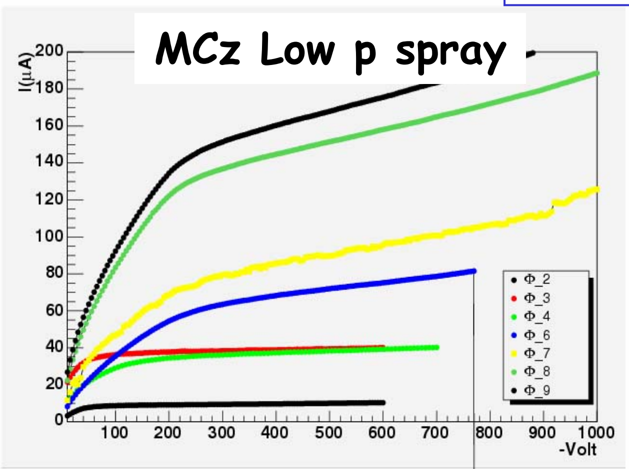

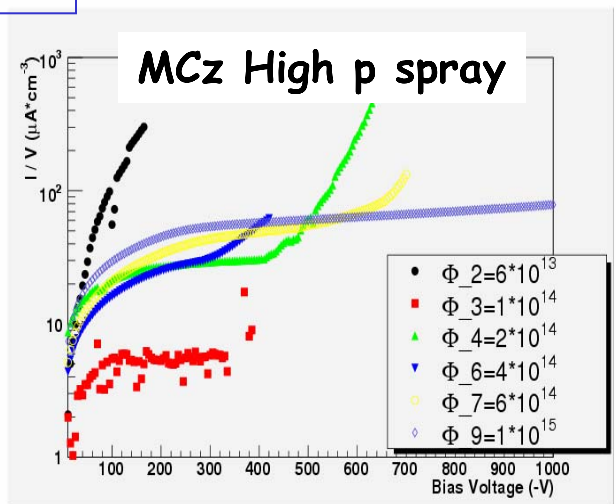

Sensors with low p-spray have IV performance comparable with n-type detectors.

Detectors with a high p-spray show improved IV performance at fluence > 4.0 10^{14} n_{eq}/cm^2

I_{leak} perf. of neutron irr. microstrip sensors

SMART

INFN Istituto Nazionale di Fisica Nucleare

n-type

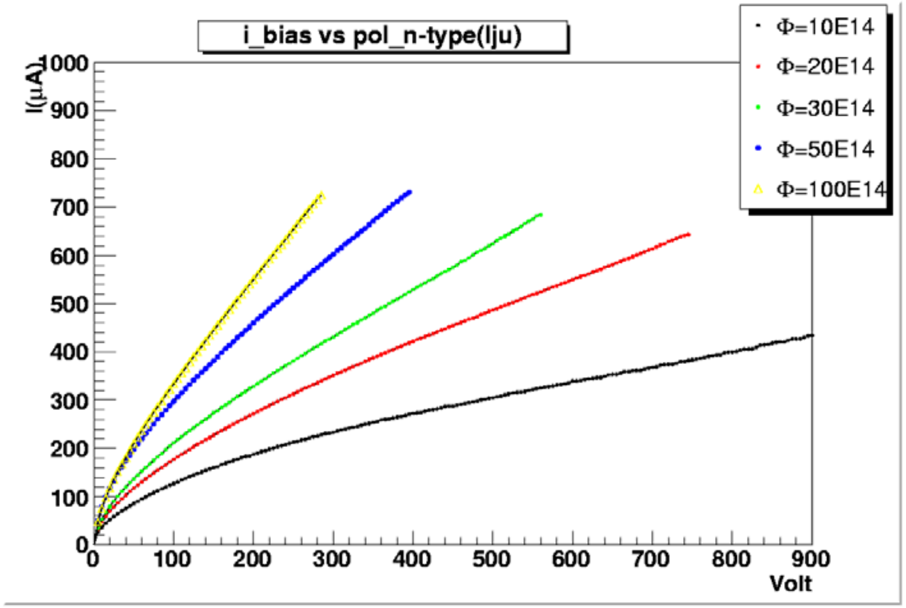

p-type

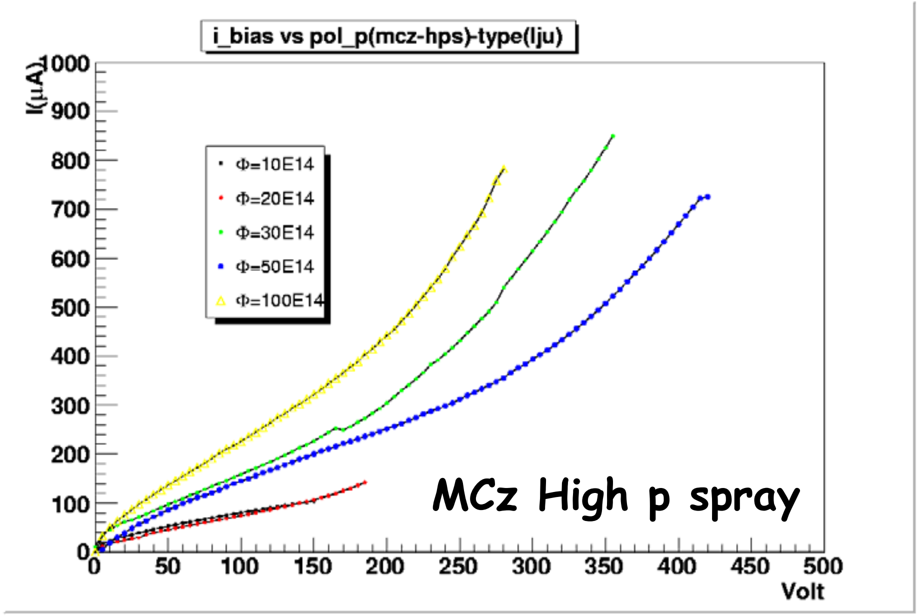

The performances of Fz and MCz p-type detectors are only slightly improved after irradiation: lower surface effects (mainly from γ contamination)

Pre Irradiation Characterization
- Minisensors (Interstrip Capacitance) -

✓Good performances of the **n-type** detectors (interstrip capacitance depends, as expected, on the minisensors geometry: strip width, pitch, metal overhang…)

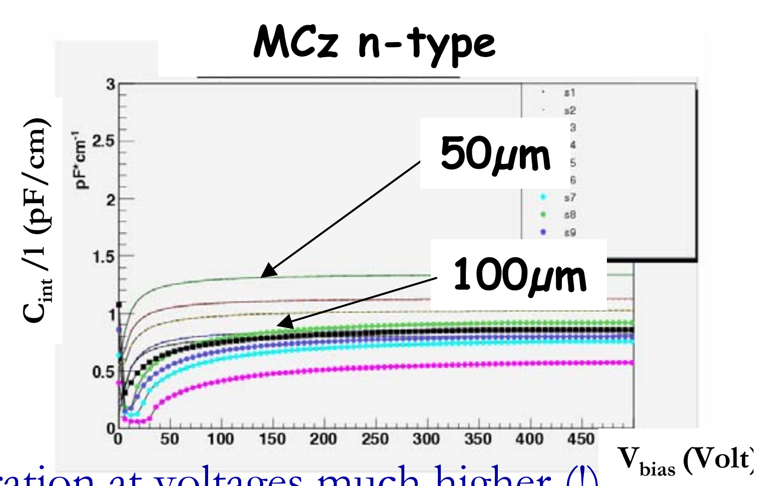

✓ Different behaviour for the **p-type** detectors:

Interstrip capacitance decreases with V_{bias} reaching saturation at voltages much higher (!) than depletion (~100V), due to the existence of mobile charge in the undepleted p-spray. The saturation is faster in low p spray and for high pitches. No differences between Fz and MCz.

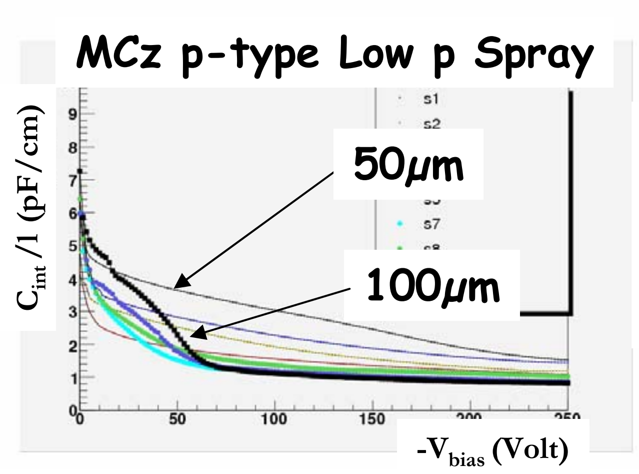

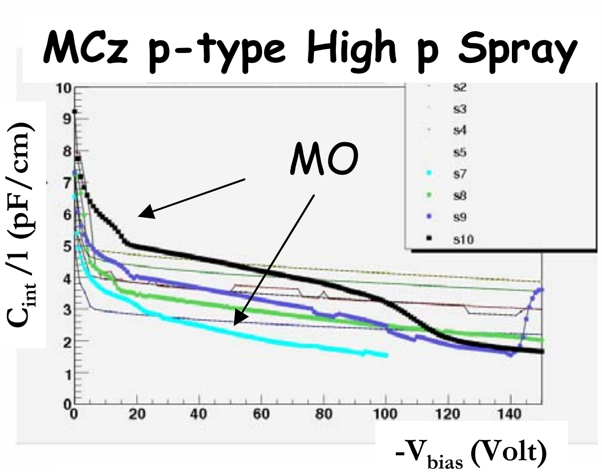

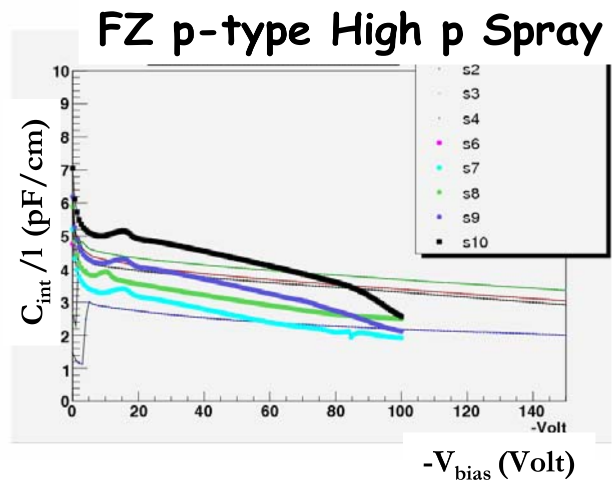

SMART

Interstrip Capacitance: proton irr.

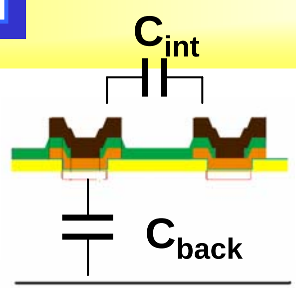

$$C_{tot} = C_{back} + 2(C_{int}\ 1^{st} + C_{in}\ 2^{nd} + \ldots)$$

Total capacitance to input amplifier

n-type

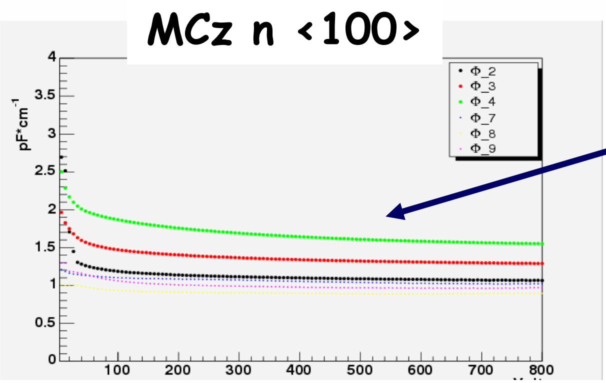

OK

pre irradiation values Recovered

Typical of <111> Si

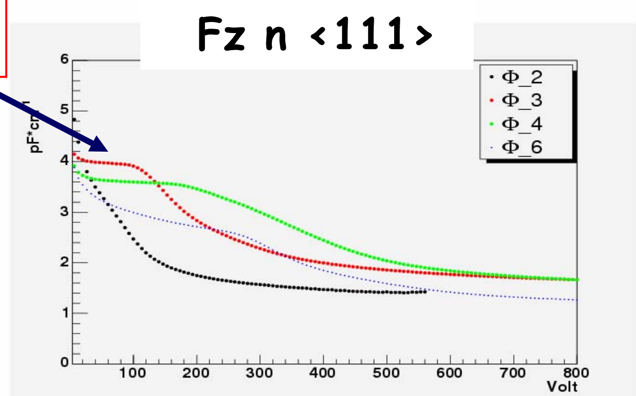

p-type

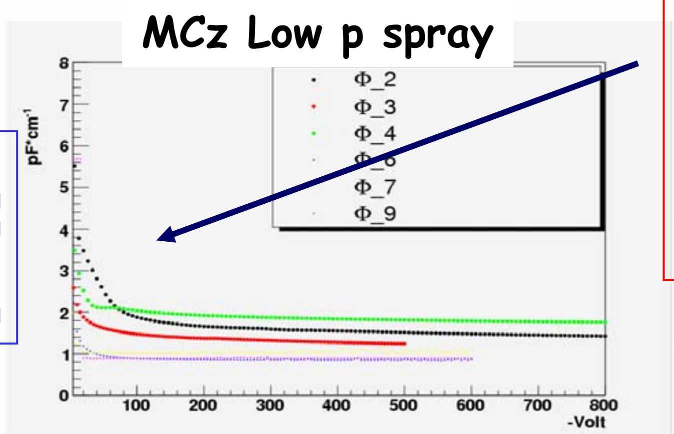

Same problem (slow saturation) found for not irradiated sensors. Slightly improved after irradiation.

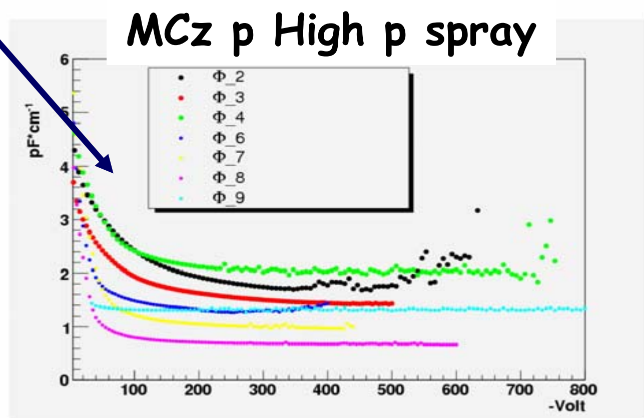

Recent devices simulation results (ITC-IRST) have shown good agreement with data: step forward in understanding strips geometry & isolation scheme

C_{int} on mini-sensors: p-type at high proton fluence

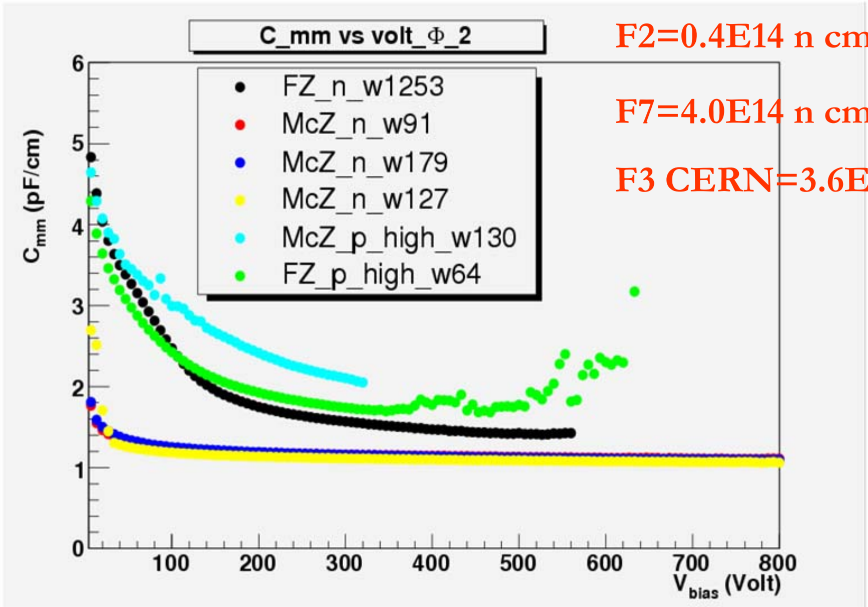

F2=0.4E14 n cm^{-2}

F7=4.0E14 n cm^{-2}

F3 CERN=3.6E15 n cm^{-2}

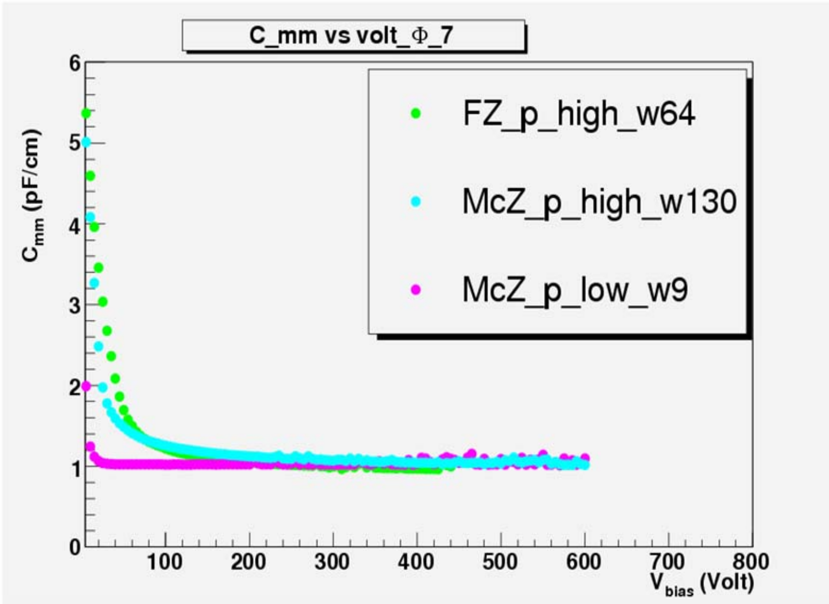

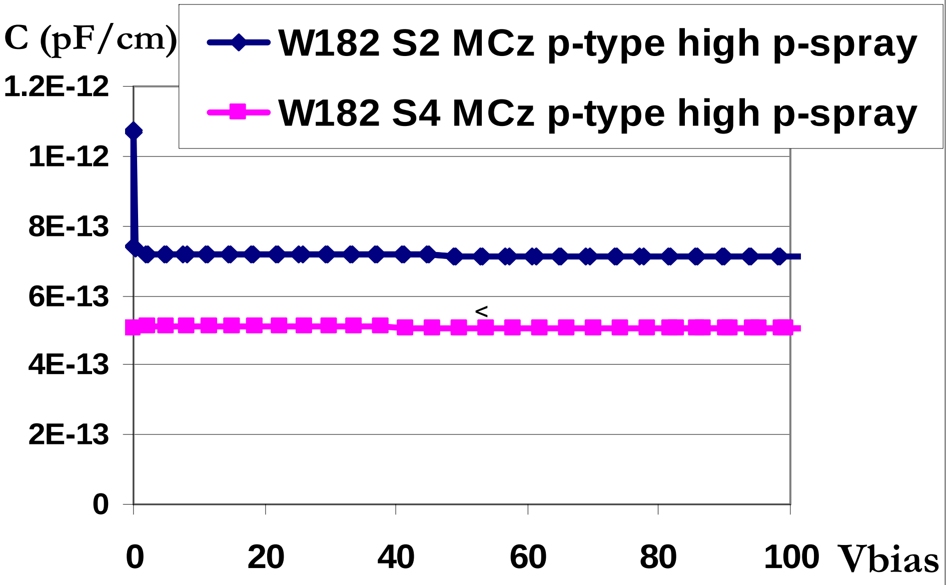

The Cint value at Φ=3.6E15 has reached the geometrical value also in the case of detectors with high p-spray

From R_{int} measurements strips seem to be isolated at all the above fluences

MOS structure: V_{FB} evolution with Φ

SMART

INFN Istituto Nazionale di Fisica Nucleare

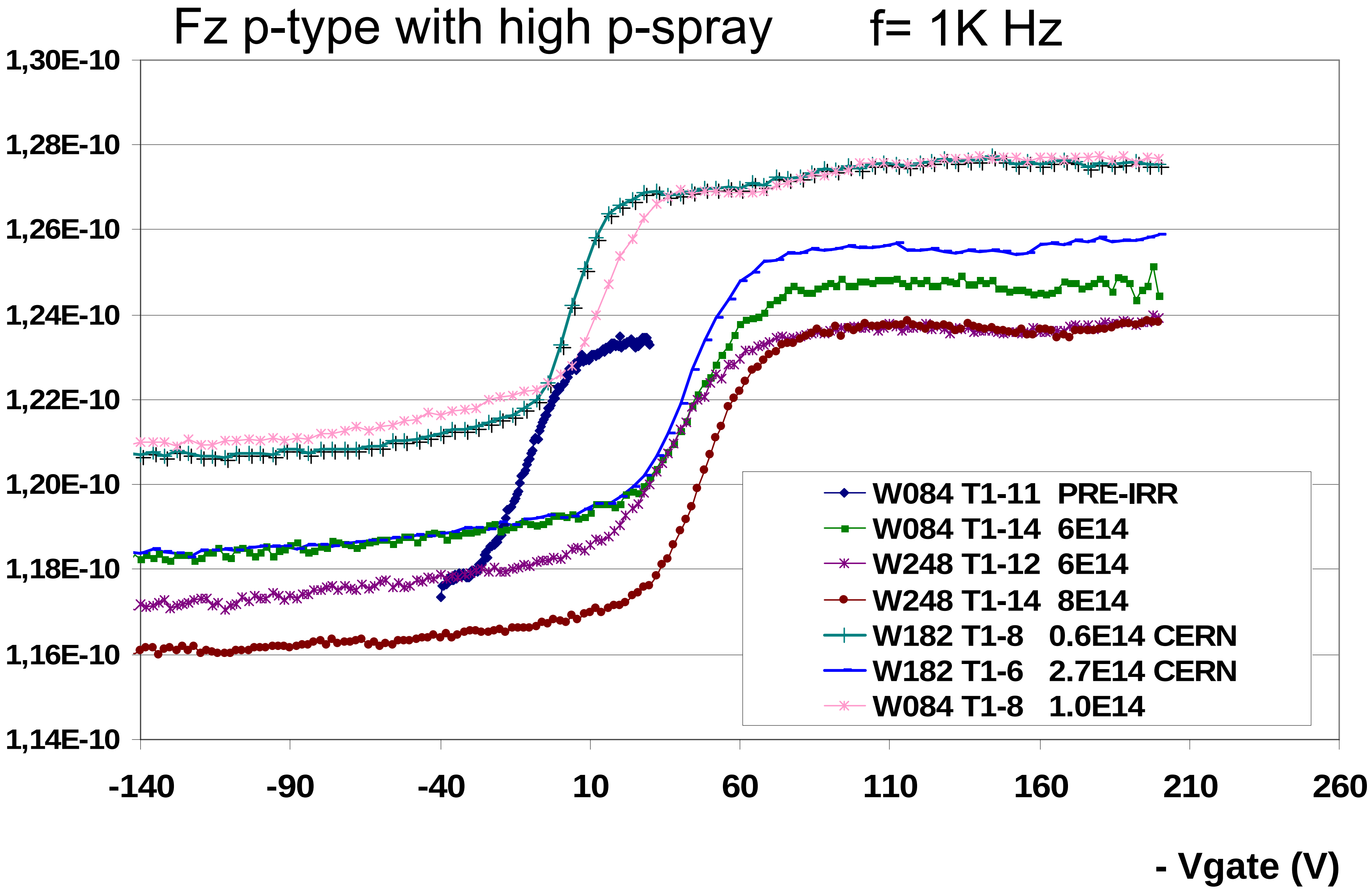

Annealing studies at 80 °C on the MOS structure

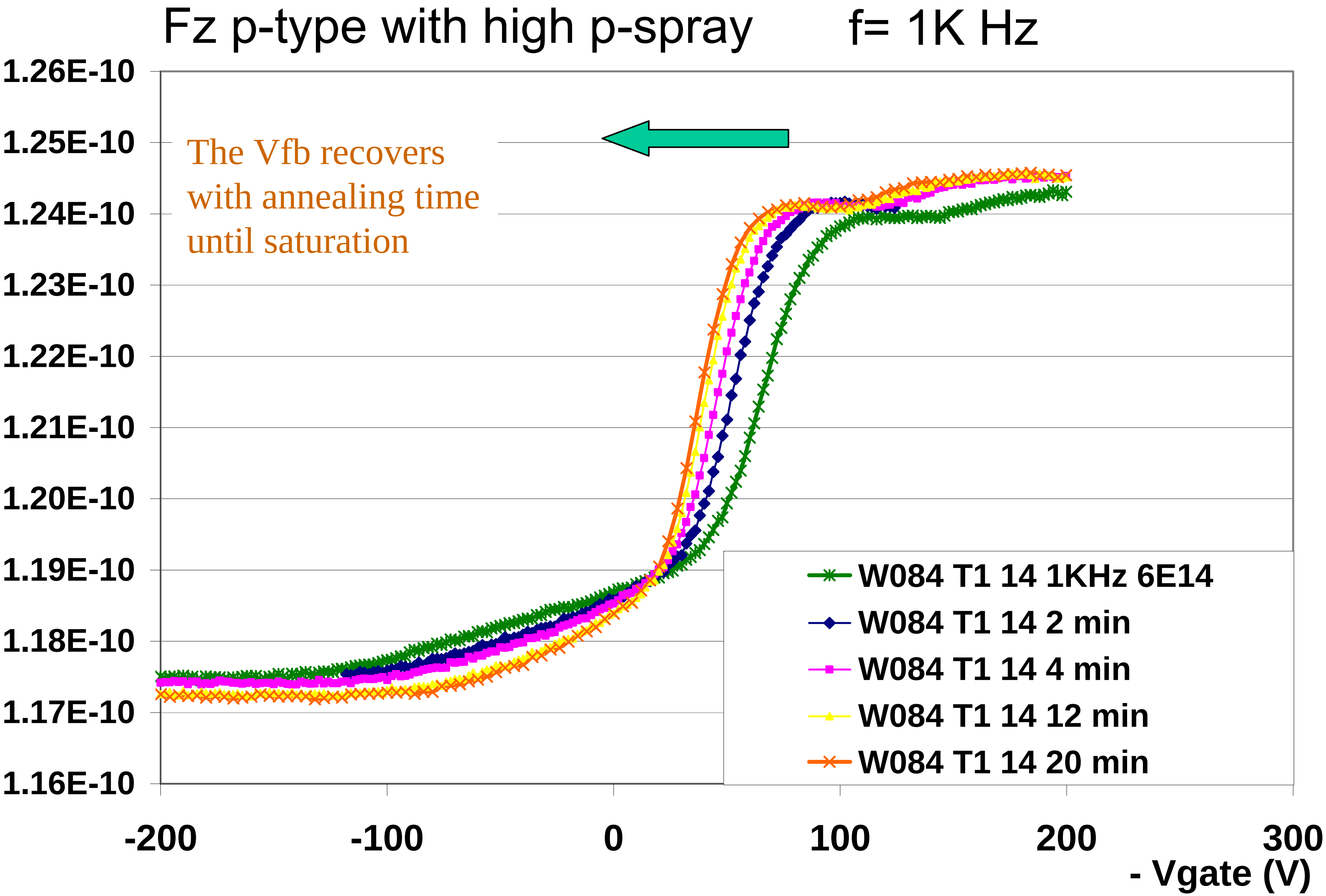

Neutron irradiation

A similar Vfb variation is observed also after neutron irradiation. Annealing studies are under way.

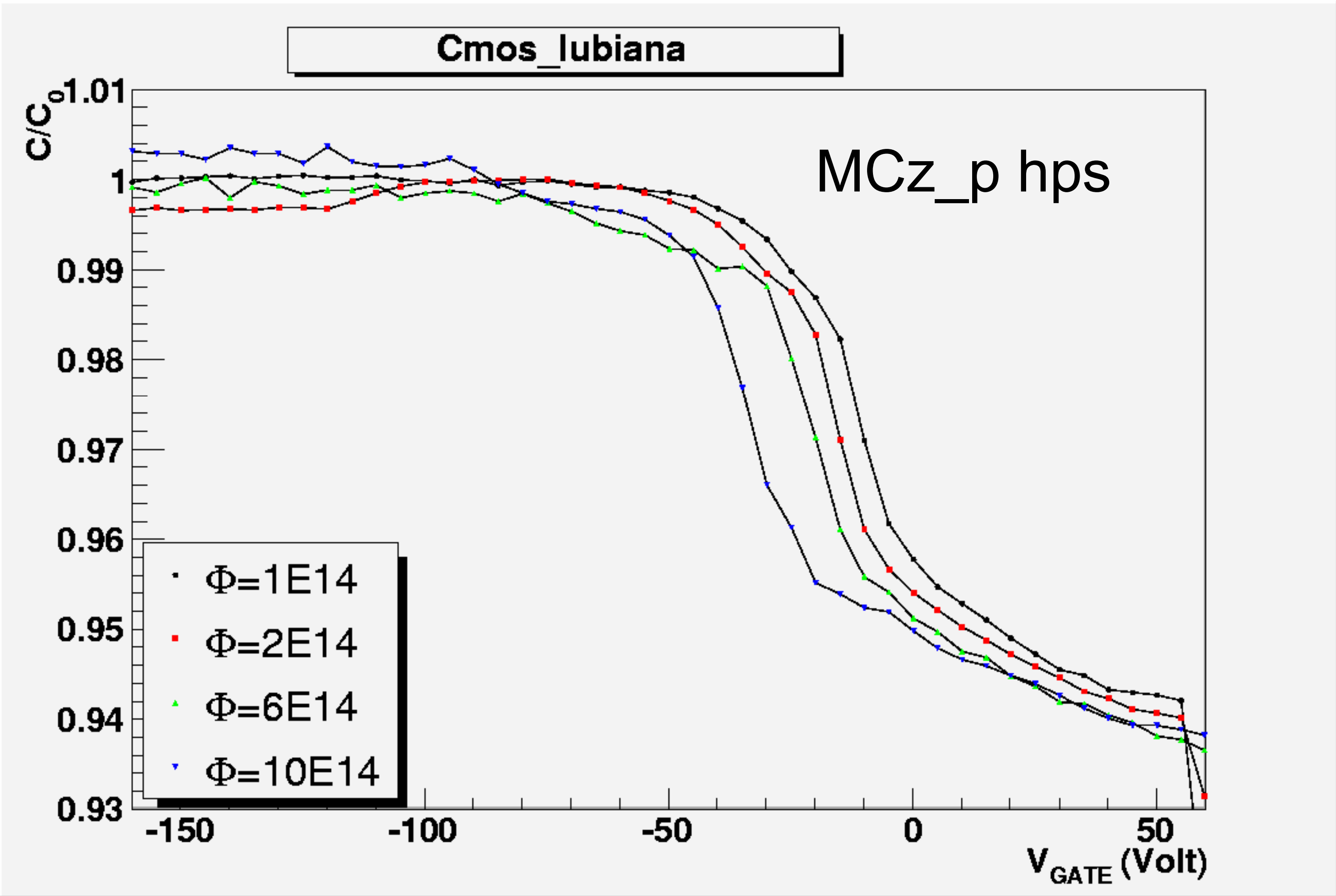

Microstrip R&D Plan: 4”

SMART

INFN Istituto Nazionale di Fisica Nucleare

Submission of 4” fabrication run in Common RD50 Project

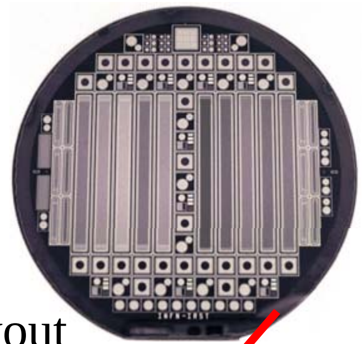

Goals:

- -a. P-type isolation study
- -b. Geometry dependence
- -c. Charge collection studies
- -d. Noise studies
- -e. System studies: cooling, high bias voltage operation,
- -f. Different materials (MCz, EPI, FZ, DOFZ)
- -g. Thickness

Materials:

- A. p-type standard FZ, of 200 and 300 μm thickness
- B. p-type DOFZ
- C. p-type MCz Si
- D. p-type EPI, with thickness > 150μm
- E. n-type MCz Si
- F. n-type EPI, with thickness > 150μm

1st draft-layout

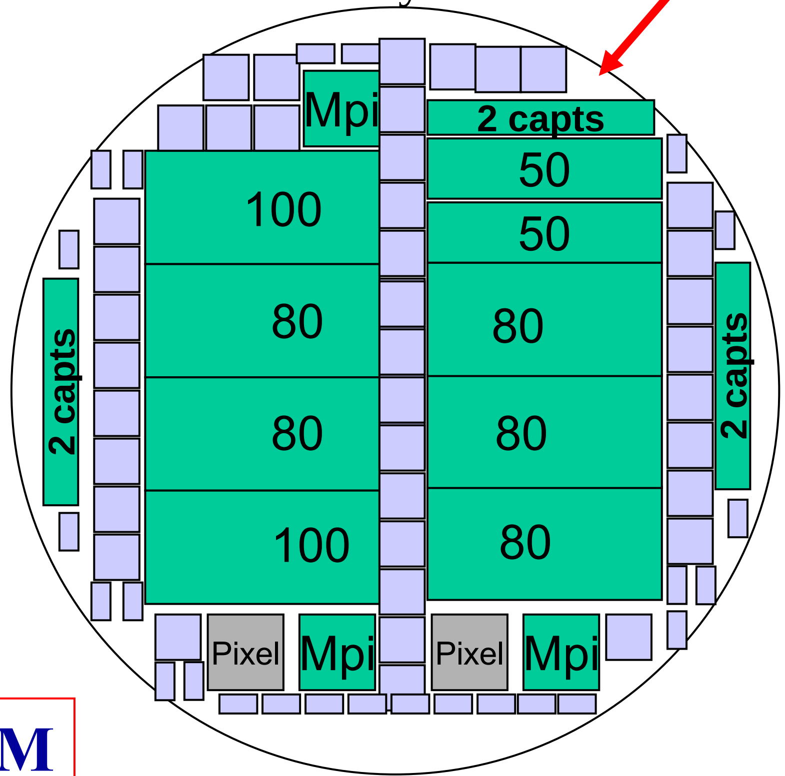

Allocated Budget: 55 Keuro

2 runs foreseen (n- & p-type)

Company : **IRST, CNM**

Details of present layout

4-inch process

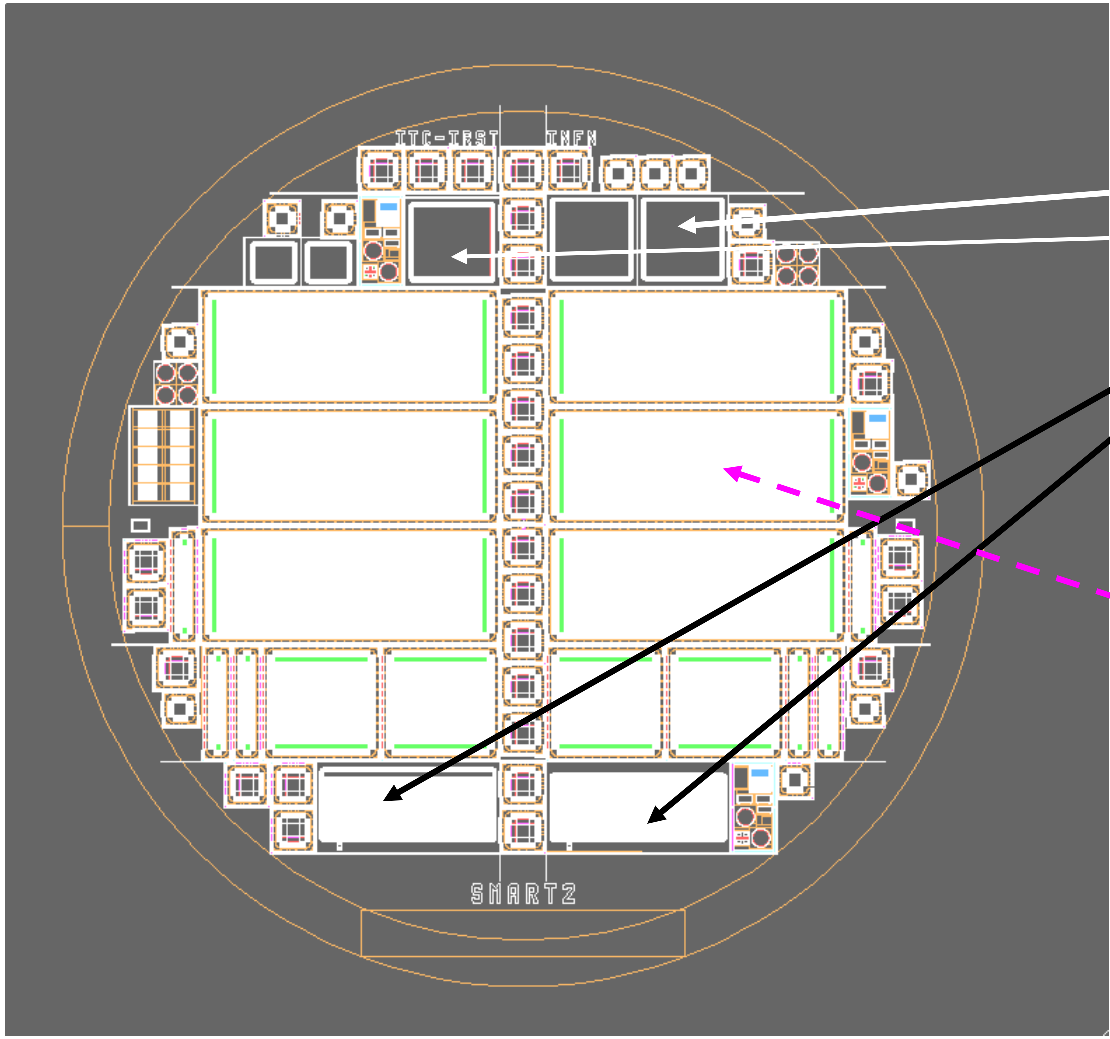

Small prototype of
1) CMS pixel
2) Atlas Pixel
3) Macro-pixel

"full size" detector
Mini-strip CMS/Atlas

Wafers ordered:
MCz, Epitaxial, FZ Si
with standard specs

Details of layout: Pixel

-Pixel CMS like on p-type bulk

-Dimension as present CMS tracker devices (100 X 150 μm^2)

-CMS-like (expensive) bump bonding

-Small size (1 chip size) : can be read-out with standard pixel electronics provided by PSI colleagues (T.Rohe)

-SS processing : n^+ on p-type

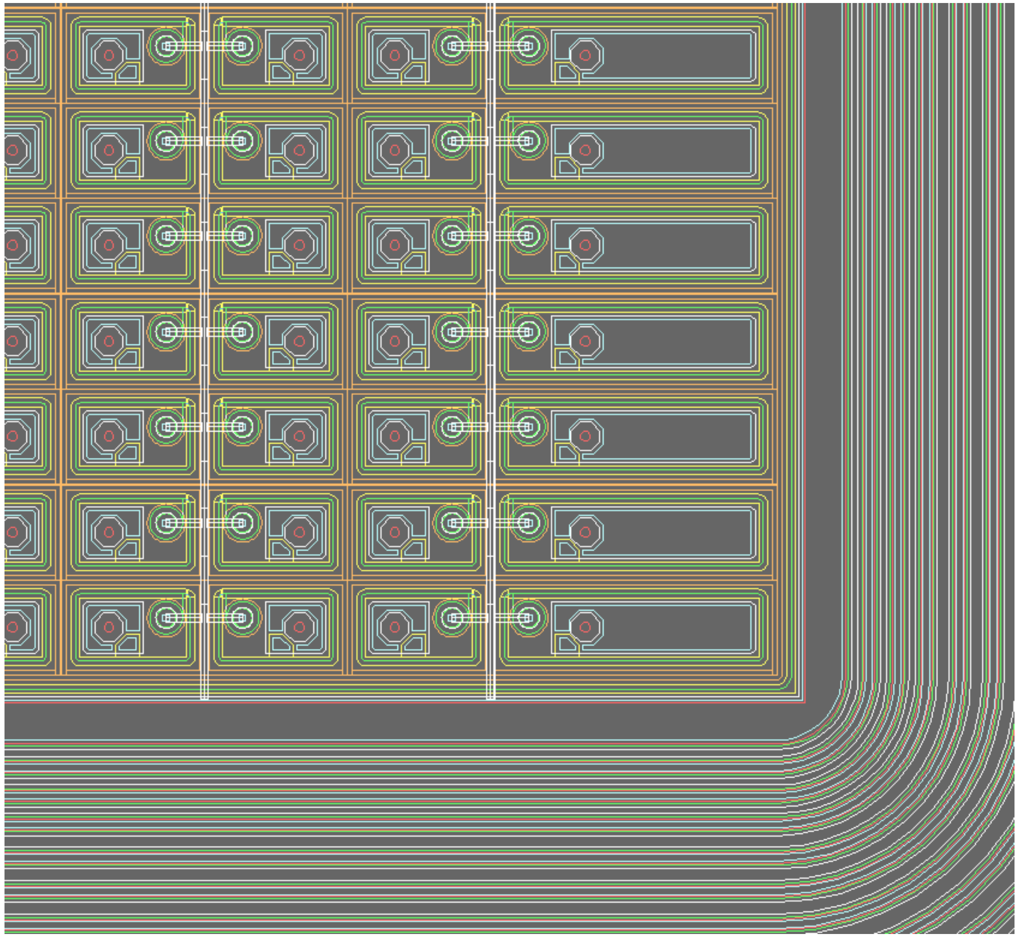

SMART Details of layout: mini-strip & macro-pixel

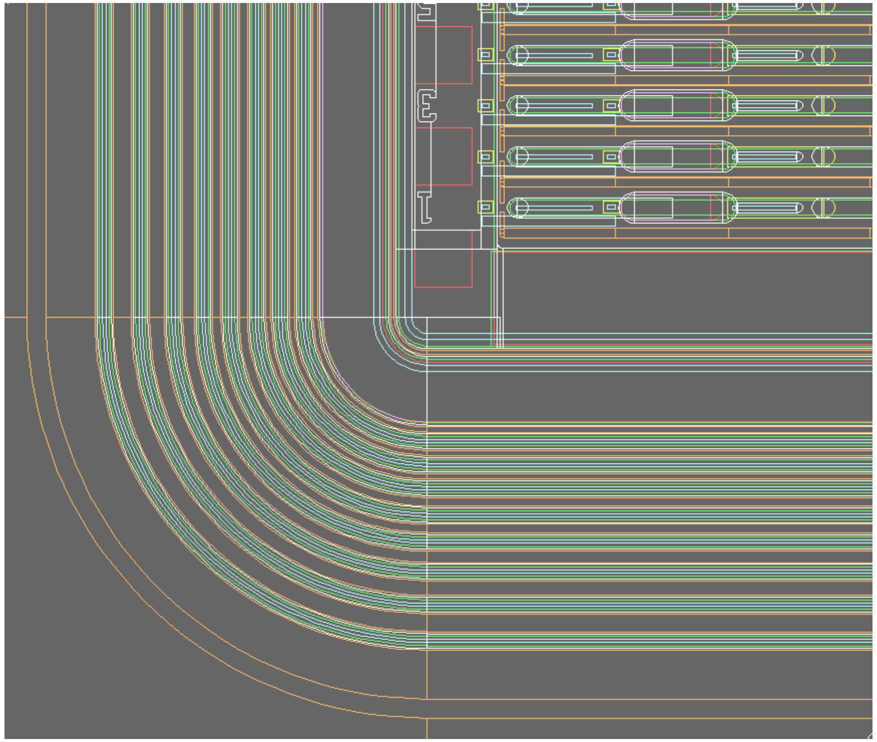

Mini-strip : 80/100 micron pitch
3 cm long

Macro-pixel : 50 micron pitch
2 cm long
Commercial bump bonding and connection routed as strip detectors (Double metal technique)